Journal of Power Sources 196 (2011) 4594–4598

Contents lists available at ScienceDirect

Journal of Power Sources

journal homepage: www.elsevier.com/locate/jpowsour

Short communication

Physical and thermal behaviour of Sr–La–Al–B–Si based SOFC glass sealants as function of SrO content and B_2O_3/SiO_2 ratio in the matrix

Prasanta Kumar Ojha[a,b,*], S.K. Rath[a,b], T.K. Chongdar[a], N.M. Gokhale[a], A.R. Kulkarni[b]

[a] Naval Materials Research Laboratory, Addl. Ambernath, Thane, Maharashtra, India
[b] Indian Institute of Technology Bombay, Mumbai, India

ARTICLE INFO

Article history:
Received 5 October 2010
Received in revised form
20 December 2010
Accepted 2 January 2011
Available online 18 January 2011

Keywords:
Network structure
Modifier
Glass transition temperature
Dilatometric softening point
Coefficient of thermal expansion
Solid oxide fuel cell

ABSTRACT

A series of SOFC glass sealants with composition SrO (x), La_2O_3 (15), Al_2O_3 (15), B_2O_3 ($40-x$), and SiO_2 (30) [x = 10, 15, 20, 25 and 30] (wt.%) [SLABS] are investigated for their structure property correlations at different compositions. Quantitative Fourier transform infrared spectroscopy shows structural rigidity with increasing SrO content, as demonstrate by an increase in the Si–O–Si/O–Si–O bending and B–O–B stretching frequencies. The role of SrO as a modifier dominates the control of the structure and behaviour of glasses compared with the effect of network formers, i.e., the B_2O_3/SiO_2 ratio. Consequent to the structural changes, increasing substitution of B_2O_3 by SrO the glasses causes increases in the density, glass transition temperature and dilatometric softening point. On the other hand, the crystallization temperatures show a decreasing trend and the coefficient of thermal expansion increases with increase in substitution.

1. Introduction

A solid oxide fuel cell (SOFC) is an electrochemical device which produces electrical energy from the chemical energy of fuel gases. Mostly, SOFCs are used as stationary power sources with power ranges from several kilowatts to several megawatts [1] depending on their use in domestic to the power grid applications. Due to such a wide variety of applications, SOFCs come in different sizes and configurations. Planar and tubular designs are common, but the most recognized cell design is planar type because of its high volumetric power density and low cost [2]. In a planar SOFC, gas-tight sealing is required along the edges of the electrodes, electrolyte and interconnect. Sealant is also used between cells to bond the cell stacks. A sealant material in a planar SOFC not only prevents intermixing of the fuel gas with the oxidant, but also provides electrical insulation between cells. To have such properties, the sealant should seal the adjacent components, should be compatible with adjoining components and most importantly the seal needs to be physically, chemically and thermally stable over long-term cell operation [3,4]. Several candidate materials are available can be broadly categorized into three types: compressive seals, compliant seals, and rigid-bonded seals. Rigid bonded seals have shown many advantages compared with compressive and compliant seals and are therefore preferred for SOFCs. These are basically glass or glass ceramics which adhere to cell components by chemical bonding and provide hermatic sealing. The advantage of rigid-bonded seals is that above the glass-softening temperature they soften, flow and seal the interfaces of cell components hermitically.

In glass seals, the desired properties such as glass transition, softening point and coefficient of thermal expansion can be tailored by selecting suitable compositions. Moreover, glass-based seals are easy to manufacture and are cost-effective. Several reports are available in the literature on rigid-bonded seals based on borate, phosphate and silicate compositions and their suitability as sealants in SOFCs has been investigated [5–14]. In these reports, glasses with different compositions have been characterized for their thermal properties, electrical properties, chemical stability and sealing behaviour, and the values have been evaluated for SOFC operational requirements.

Although glass-based seals have several desirable features, achieving all the required properties like high coefficient of thermal expansion (CTE) and prolonged thermal and chemical stability is a difficult task. Also, glass-based seals have poor resistance to thermal cycling and other static and dynamic forces. To address such issues researchers are continuously trying to understand the basics of glass science and sealing technology. Attempts are also

* Corresponding author at: Naval Materials Research Laboratory, Ministry of Defence, Govt of India, Shil Badlapur Road, Anand Nagar P.O., Ambarnath (E), Thane, Maharashtra 421506, India. Tel.: +91 251 2623219; fax: +91 251 2623004.
E-mail address: pkojha77@yahoo.co.in (P.K. Ojha).

0378-7753/$ – see front matter © 2011 Elsevier B.V. All rights reserved.
doi:10.1016/j.jpowsour.2011.01.021

being made to determine the factor that control glass behaviour. It has been shown that the behaviour of glass sealants depends on their composition and atomic arrangement in the glass network structure. The glass structure is very complex and not fully understood. In general, the glass is comprise of three main components: network formers, network modifiers, and intermediate oxides. In some cases, minor additives are added to control the properties. Common glass formers for SOFC seals are SiO_2 and B_2O_3. Cations of these network formers act as the centres of polyhedral units. Network modifiers are alkaline oxides such as Li_2O, Na_2O and K_2O and alkaline earth oxides like BaO, SrO, CaO and MgO. Network modifiers provide additional oxygen atoms to modify the structure, where as charge neutrality in the structure is maintained by random positioning of the cations in the polyhedral network. Thus with introduction of network modifiers, the bridging and non-bridging content of the network is modified and the properties of glasses are changed. Up to a certain extent, additives behave in a similar fashion in the glass network. Intermediate oxides such as Al_2O_3 and Ga_2O_3 have cations with higher valency and lower coordination number. These oxides behave as conditional glass formers, i.e., glass formers if they participate in the glass network, and as glass modifiers if not. Therefore, the glass behaviour depends the structure and functionality of different oxides present in the composition. In this regard, several reports are available in which glass structures have been elucidated for different compositions using techniques such as FTIR, Raman and MAS-NMR spectroscopy [15–18]. All these reports focus on the structural findings with respect to the composition of glasses and not with the properties of glasses for sealing applications in SOFC. Similarly, there are reports [5–14] that consider the compositions of different glasses with no attention to the structural aspects. At present, most of the available reports on SOFC sealing glass science and technology highlight either composition structure correlation. In this study, however, the composition structure and properties correlated systematically for a series of SOFC glass sealants. Which have been developed based on the composition SrO, La_2O_3, Al_2O_3, B_2O_3 and SiO_2 using a melt quench technique. A new approach of quantitative FTIR is used for the determination of the structural changes of glasses as a function of composition. The glass properties have been evaluated using density measurement and thermal analysis. Different properties of glasses are compared and correlated with the structural findings and functionality of the component oxides in the glass matrix.

2. Experimental

Glasses were prepared by a melt quench technique using SrO (x wt.%), La_2O_3 (15 wt.%), Al_2O_3 (15 wt.%), B_2O_3 ($40 - x$ wt.%) and SiO_2 (30 wt.%) for x = 10, 15, 20, 25 and 30. For glass making, SiO_2, Al_2O_3 and La_2O_3 were used as oxides. Boric acid (H_3BO_3) was used as the source for B_2O_3 and $SrCO_3$ for SrO. All the chemicals were analytical reagent (AR) grade and procured from Indian sources and used as obtained. Batch formulations were calculated carefully considering the gravimetric factors for H_3BO_3 and $SrCO_3$. Raw materials in appropriate proportions for a 50 g batch size were mixed thoroughly. The total mass was melted in a platinum crucible and quenched in a pre-heated mould. Subsequently, the glasses were annealed at 50 °C below their glass transition temperatures for removal of thermal stresses during formation.

To confirm the glassy phase, melt quench samples were characterized by X-ray diffractometry (XRD) using XPert MPD, PAnalytical in the range of 20–80° (2θ) with a step size of 0.005° and Cu K_α radiation. Fourier transform infrared (FTIR) spectroscopy of glass samples were carried out using a 1600 Series Perkin-Elmer instrument via the KBr pellet technique method in the range of 400–4000 cm^{-1}. The spectra were corrected using two-point baseline correction, normalized to eliminate the concentration effect of the powder sample in the KBr disc. To obtain quantitative information about structural groups, the spectra were deconvoluted in Gaussian bands. Only the 400–1600 cm^{-1} range was considered for deconvolution and the least-squares method was used to analyze the graphs. Data generated by deconvolution include peak position, peak height, FWHM of the peak, and area under the peak. Peaks were assigned for characteristic bands, and relative areas under the peaks were calculated with respect to the total area under all peaks. The relative area gives a quantitative idea of the corresponding structural group in the glass structure. The FTIR spectra of all the glass samples were deconvoluted and the generated data were analyzed for structural findings. To evaluate the physical properties, the densities of glass samples were measured using a helium gas pycnometer (Quanta crome, Ultra Pycnometer 1000, USA). Differential thermal analysis (DTA) of the glass samples was performed in air (Setsys 16, SETARAM, France) at a heating rate of 5 °C min^{-1} to determine the thermal behaviour. The coefficient of thermal expansion (CTE) of each glass was measured with a dilatometer (UNITHERM™ MODEL 1161 Dilatometer System, Anter Corporation, USA) operated at a heating rate of 3 °C min^{-1} with cylindrical samples of length ~15 mm and a cross-sectional diameter of 5–7 mm.

Table 1
Batches for glass-making with composition and nomenclature.

Glass code	Glass composition (wt.%)					Density (gcc^{-1})
	La_2O_3	Al_2O_3	SiO_2	SrO	B_2O_3	
SLABS-3	15	15	30	10	30	2.67
SLABS-4	15	15	30	15	25	2.92
SLABS-5	15	15	30	20	20	3.01
SLABS-6	15	15	30	25	15	3.11
SLABS-7	15	15	30	30	10	3.32

3. Results and discussion

The different batch compositions used to prepare the glasses and the nomenclature for each composition are listed in Table 1. Each glass was prepared in a rectangular slab shape, and was transparent and free of bubbles or cracks. Phase analysis by XRD shows that plots of all samples lack high-intensity peaks; but a broad hump appears in each case and this is a clear indication of the amorphous/glassy nature of the sample.

In the glass composition the network former B_2O_3 is partially substituted by network modifier SrO. Thus the resulting behaviour of the glasses is a combined effect of both. In general, for glass systems having both B_2O_3 and SiO_2 as network formers the properties are interpreted against the B_2O_3/SiO_2 ratio. The content of network modifier in the matrix also affects the properties as it controls glass structure. In this series of glasses, as B_2O_3 is systematically substituted by SrO, hence the B_2O_3/SiO_2 ratio in the glass changes along with SrO content. In the series, from SLABS-3 to SLABS-7 the B_2O_3/SiO_2 ratio decreases from 1 to 0.33 whereas the SrO content increases from 10 to 30 wt.%. Therefore, for a true interpretation of structure property correlation all the following data are presented against both the variables.

For structural investigation, the glass samples were characterized through FTIR spectroscopy; the spectra were deconvoluted and analyzed. It was stated in a previous report [19] that structure analysis by FTIR indicates two types of network structures in the glass: one that consists of BO_3 and BO_4 units and the other of in SiO_4 units. Also, it was observed that with increase in SrO content, i.e., decreasing B_2O_3/SiO_2 ratio in the matrix, the connectivity of the glass network decreases with generation of more non-bridging oxygens. In the present study, deconvoluted data for the charac-

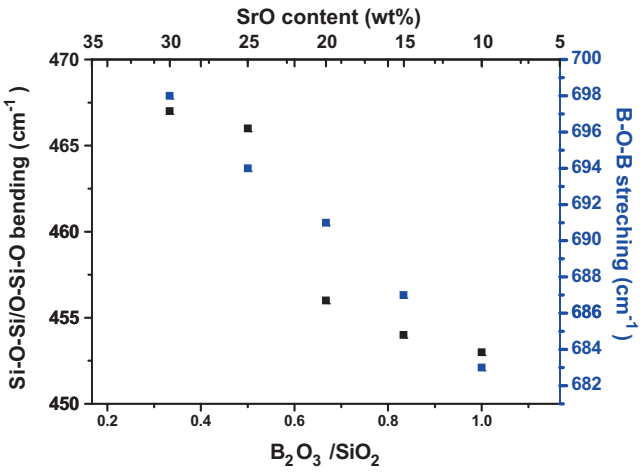

Fig. 1. Variation of Si–O–Si/O–Si–O bending frequency and B–O–B stretching frequency of SLABS glasses.

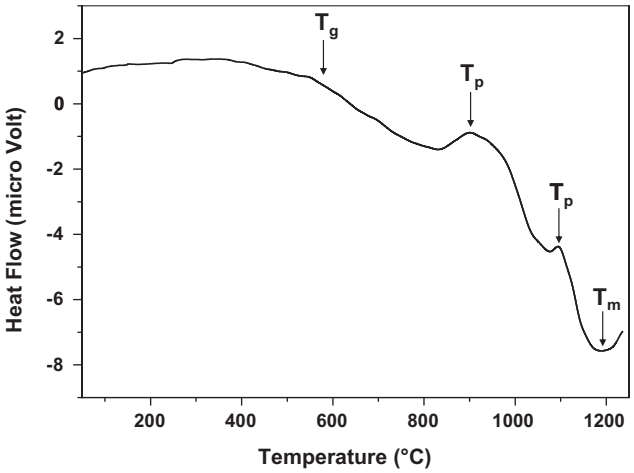

Fig. 3. DTA plot of SLABS-3 glass.

teristic bond vibration frequencies of Si–O–Si/O–Si–O bending and B–O–B stretching vibrations of the glass networks are shown in Fig. 1 against the compositions of the glasses. The Si–O–Si/O–Si–O bending frequency and B–O–B stretching frequency increase monotonically with decrease in B_2O_3/SiO_2 ratio and increase in SrO content in the glass. The bending frequency increases from 453 to 467 cm^{-1} from SLABS-3 to SLABS-7. Similarly, the B–O–B stretching frequency increases from 683 to 698 cm^{-1} from SLABS-3 to SLABS-7. This indicates that the structure becomes rigid and thereby requires more energy to bending and stretching of bonds. Lu et al. [20] have reported that the glass network connectivity increases with decreasing B_2O_3/SiO_2 ratio in a SLABS system. In the present case 'however' it is observed that even if the ratio decreases from 1 to 0.333, the connectivity decreases with more network breakage. This may be due to network modifiers having more impact over glass formers such as SiO_2 and B_2O_3 [21]. Such an observation of decreasing connectivity with increasing SrO content in the glass matrix indicates that SrO acts as a network modifier and hence inverts the structure by breaking the network bonds in the SiO_4 tetrahedral. In the broken network, the Sr^{2+} ions occupy interstitial positions surrounded by non-bridging oxygen ions.

A similar observation is made by measuring the densities of glasses, as shown in Fig. 2. The density increases from 2.67 to 3.32 gcc^{-1} for glass samples from SLABS-3 to SLABS-7, and thereby reflects the compactness of the structure. Increasing connectivity makes the glass structure open so that the density decreases. An increasing density signifies compactness of the structure due to network breakage with increasing SrO content, despite the decreasing value of the B_2O_3/SiO_2 ratio.

Thermal analysis of the glass samples was carried out using DTA and dilatometry. A typical DTA plot of SLABS-3 glass is shown in Fig. 3 and displays a glass transition temperature (T_g), two exothermic peaks assigned to be devitrification temperatures (T_p) and an endothermic melting peak (T_m). The DTA plots of all glasses are found to be similar in nature. Plots of linear expansion against temperature, obtained from a dilatometer, are presented in Fig. 4 for three glass compositions. The coefficient of thermal expansion (CTE) of each glass sample is calculated using the software from the slope of the expansion curve and the sample dimension. CTEs of glasses against their compositions are shown in the inset of Fig. 4. In the linear expansion curve, the temperature with sudden change in expansion has been assigned as dilatometric glass transition (T_g) and the temperature of maximum expansion as the softening point of glass (T_s). Glass transition temperatures (T_g) of glasses obtained from DTA analysis and softening temperatures (T_s) obtained from dilatometric data are plotted against the compositions of glasses in Fig. 5. Both the glass transition temperature and softening temperature decreased with increasing B_2O_3/SiO_2 ratio and decreasing

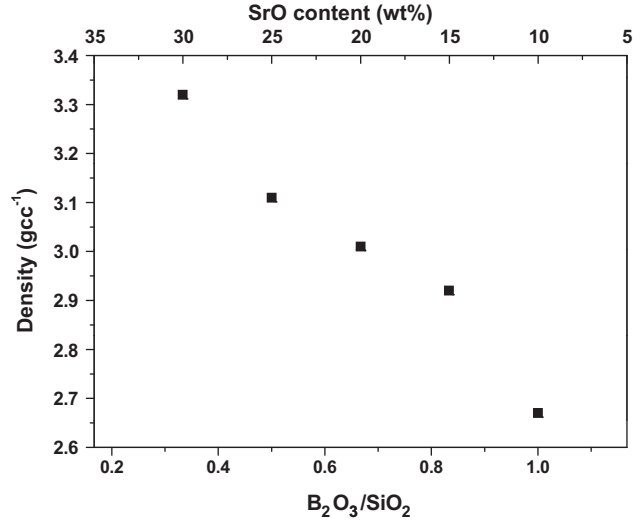

Fig. 2. Density of SLABS glasses.

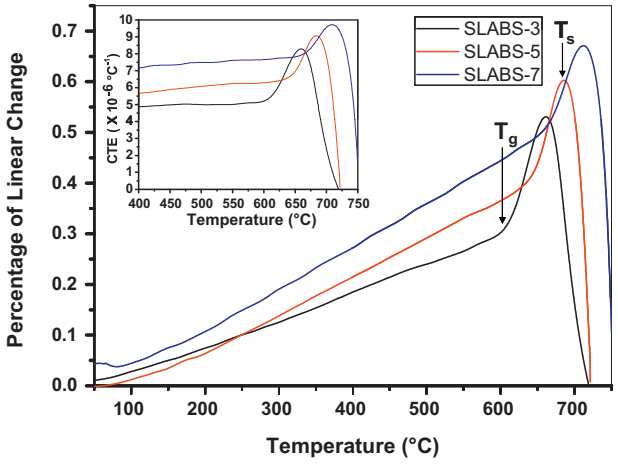

Fig. 4. Dilatometer plots of SLABS-3, SLABS-5 and SLABS-7 samples with coefficient of thermal expansion (CTE) plots shown in the inset.

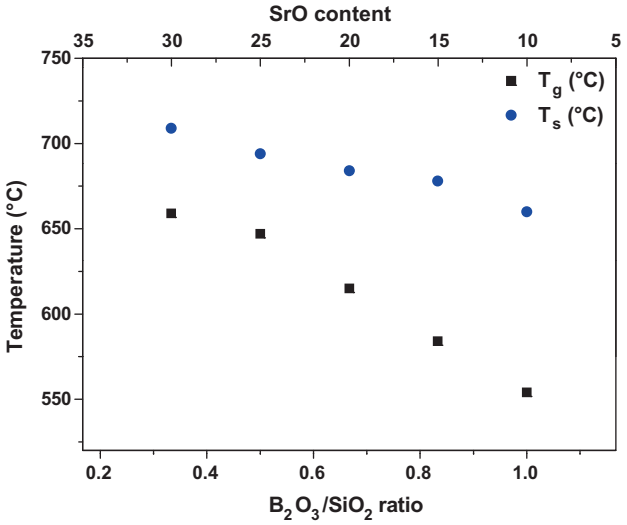

Fig. 5. Glass transition and softening temperature of SLABS glasses.

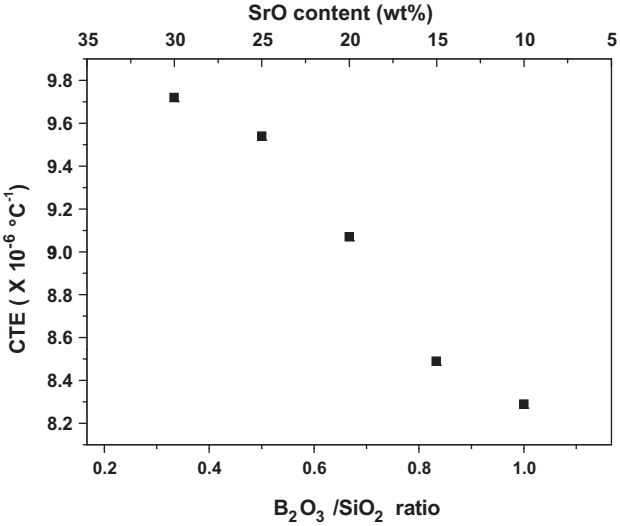

Fig. 7. Coefficient of thermal expansion (CTE) of SLABS glasses.

SrO content in the matrix. In borosilicate glasses, T_g and T_s both decrease with increase in B_2O_3/SiO_2 ratio because B_2O_3 lowers the glass viscosity and the network rigidity. Moreover, B_2O_3 increases the non-bridging oxygen-containing silicate structural units and trigonal boroxyl groups. These structural degrade the glass network connectivity and thus T_g and T_s [6,7,22–24]. Along with the effect of B_2O_3/SiO_2 ratio, increasing SrO content in the matrix leads to an increase in NBO content due to network breakage and results in an increase in T_g and T_s. Hence in the series of glasses from SLABS-3 to SLABS-7, T_g increases from 554 to 659 °C and T_s increases from 660 to 709 °C. In DTA, it is also observed that each glass on heating shows two devitrifications. The devitrification temperature varies from glass to glass. In the series of glasses from SLABS-3 to SLABS-7, the first devitrification temperature decreases from 913 to 821 °C and the second devitrification temperature decreases from 1092 to 1021 °C. The two devitrification temperatures as observed from DTA analysis are plotted against composition in Fig. 6. This shows that devitrification temperatures decrease with decreasing B_2O_3/SiO_2 ratio and increasing SrO content. This is also a clear indication of network breakage due to increasing modifier content that favours the thermodynamics of the devitrification process and thereby lowers the devitrification temperature.

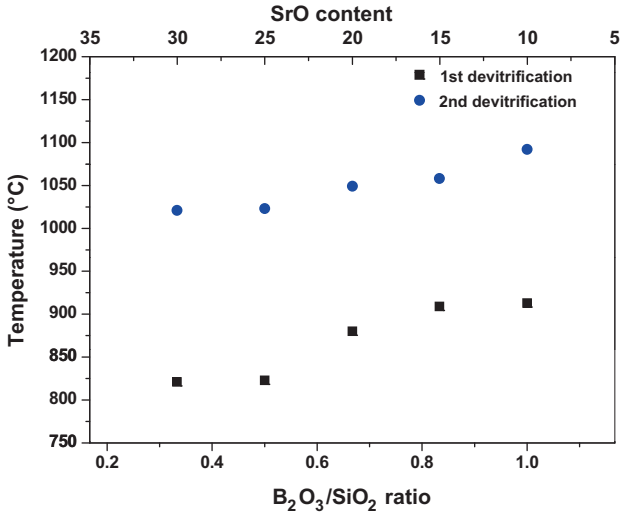

Fig. 6. Devitrification temperatures of SLABS glasses.

The dilatometric data of glasses are presented in Fig. 7 against the glass composition. The plots show that at a higher SrO concentration or at a lower B_2O_3/SiO_2 ratio, the glasses expand more at higher temperatures. The coefficient of thermal expansion of glasses calculated from the expansion data increases gradually from $8.29 \times 10^{-6}\,°C^{-1}$ for SLABS-3 to $9.72 \times 10^{-6}\,°C^{-1}$ for SLABS-7. The CTE of a seal glass depends on the glass structure symmetry, bond bending and molar free volume. For example, pure SiO_2 glass has a CTE of $0.6 \times 10^{-6}\,°C^{-1}$ due to its high symmetry and B_2O_3 has a CTE of $14.4 \times 10^{-6}\,°C^{-1}$ due to its low symmetry [25]. Modifiers in silicate glasses create non-bridging oxygen (NBO) species that decrease the average symmetry of the Si–O bonds and thus increase the CTE [26]. CTE also increases if the molar free volume and bond bending of glass decrease [25]. For this series of glasses, increasing SrO content results in an increasing network breakage, thereby generating more NBO, which also results in decreasing bond bending due to the rigidity of the structure as mentioned in the FTIR results. Hence the CTEs of the glass samples increase with increase in SrO content despite a lowering of the B_2O_3/SiO_2 ratio.

4. Conclusions

A series of glass sealants for SOFC application are prepared by melt quench technique with compositions SrO (x wt.%), La_2O_3 (15 wt.%), Al_2O_3 (15 wt.%), B_2O_3 ($40 - x$ wt.%) and SiO_2 (30 wt.%) [x = 10, 15, 20, 25 and 30]. Characterization by FTIR, density measurements and thermal analysis shows that the effect of SrO is dominant as a network former, i.e., B_2O_3/SiO_2 ratio. Hence the glass structure is controlled by the SrO content in the matrix which, in turn, controls the behaviour of glasses. With increase in SrO content in the matrix, the structure is becomes inverted and rigid as evidenced by an increase in the stretching and bending frequencies of bond vibrations. This structural change is reflected in the properties of the glasses. The densities of the glasses are found to increase with increasing SrO content and decreasing B_2O_3/SiO_2 ratio. Increasing SrO and decreasing B_2O_3/SiO_2 ratio result in increases in the glass transition temperature and in the softening temperature. These structural changes favour the crystallization process and lead to a lowering of the crystallization temperature. On the other hand, the thermal expansion increases which results in a higher CTE.

References

[1] D. Stolten, L.G.J.B.D. Haart, L. Blum, Ceram. Eng. Sci. Proc. 24 (2003) 263.

[2] A. Weber, E. Ivers-Tiffée, J. Power Sources 127 (2004) 273.
[3] K.S. Weil, J. Mier, Met. Mater. Soc. 58 (2006) 37.
[4] J.W. Fergus, J. Power Sources 147 (2005) 46.
[5] K.D. Meinhardt, J.D. Vienna, T.R. Armstrong, L.R. Pederson, U.S. Patent 6,532,769 (March 18, 2003).
[6] K.L. Ley, M. Krumpelt, R. Kumar, J.H. Meiser, I. Bloom, J. Mater. Res. 11 (1996) 1489–1493.
[7] S.-B. Sohn, S.-Y. Choi, G.-H. Kim, H.-S. Song, G.-D. Kim, J. Am. Ceram. Soc. 87 (2004) 254–260.
[8] R.E. Loehman, H.P. Dumm, H. Hofer, Ceram. Eng. Sci. Proc. 23 (2002) 699.
[9] K. Eichler, G. Solow, P. Otschik, W. Schaffrath, J. Eur. Ceram. Soc. 19 (1999) 1101.
[10] P. Geasee, R. Conradt, T. Schwickert, A. Janke, J. Remmel, F. Tietz, Proc. Int. Congr. Glass 2 (2001) 47 (extended abstracts).
[11] R. Zheng, S.R. Wang, H.W. Nie, T.-L. Wen, J. Power Sources 128 (2004) 165–172.
[12] Z. Yang, K.D. Meinhardt, J.W. Stevenson, J. Electrochem. Soc. 150 (2003) A1095–A1101.
[13] Z. Yang, J.W. Stevenson, K.D. Meinhardt, Solid State Ionics 160 (2003) 213–225.
[14] I.D. Bloom, K.L. Ley, U.S. Patent 5,453,331 (September 26, 1995).
[15] K. El-Egili, Physica B 325 (2003) 340–348.
[16] F. Seifert, B.O. Mysen, D. Virgo, Am. Miner. 67 (7–8) (1982) 696–717.
[17] H. Li, P. Hrma, J.D. Vienna, M. Qian, Y. Su, D.E. Smith, J. Non-Cryst. Solids 331 (1–3) (2003) 202–216.
[18] K. Glock, O. Hirsch, P. Rehak, B. Thomas, C. Jäger, J. Non-Cryst. Solids 232–234 (1998) 113–118.
[19] P.K. Ojha, S.K. Rath, T.K. Chongdar, N.M. Gokhale, A.R. Kulkarni, Mater. Chem. Phys., under review.
[20] K. Lu, M.K. Mahapatra, J. Appl. Phys. 104 (2008) 074910.
[21] P. Brix, L. Gaschler, US Patent 5,137,849 (1992).
[22] M.K. Mahapatra, K. Lu, R.J. Bodnar, Appl. Phys. A 95 (2009) 493.
[23] S.B. Sohn, S.Y. Choi, G.H. Kim, H.S. Song, G.D. Kim, J. Non-Cryst. Solids 297 (2002) 103.
[24] F. Smeacetto, M. Salvo, M. Ferraris, V. Casalegno, P. Asinari, J. Eur. Ceram. Soc. 28 (2008) 611.
[25] M.B. Volf, Glass Science and Technology, Elsevier, Amsterdam, 1984.
[26] J.E. Shelby, Introduction to Glass Science and Technology, The Royal Society of Chemistry, Cambridge, 2005.

Glossary

CTE: Coefficient of thermal expansion.
DTA: Differential thermal analysis.
FTIR: Fourier transform infrared spectroscopy.
FWHM: Full width at half maximum.
MAS-NMR: Magic Angle Spinning-Nuclear Magnetic Resonance.
SOFC: Solid oxide fuel cell.
XRD: X-ray diffractometry.